PROCEEDINGS OF SCIENCE

Transverse Single Spin Asymmetry of Electromagnetic Jets for Inclusive and Single Diffractive Processes at Forward Rapidity in $p^{\uparrow}+p$ Collisions at $\sqrt{s} = 200$ GeV at STAR

Xilin Liang, for the STAR Collaboration[a,*]

[a] *University of California, Riverside,*
900 University Ave, RIverside, CA, USA

E-mail: xilin.liang@email.ucr.edu

There have been numerous attempts, in the last decades, to unravel the origin of the unexpectedly significant transverse single-spin asymmetry (A_N) observed in inclusive hadron productions at forward rapidities in transversely polarized $p^{\uparrow}+p$ collisions across various center-of-mass energies ($\sqrt{s}$). Theoretical frameworks proposed to explain this phenomenon include the twist-3 contributions in the collinear factorization framework, the transverse-momentum-dependent contributions from the initial-state quark and gluon Sivers functions, and/or final-state Collins fragmentation functions. Furthermore, recent studies at STAR hinted that such sizeable A_N values may potentially arise from diffractive processes. We present a multi-dimensional investigation into the A_N for electromagnetic jets (EM-jets) produced in inclusive processes using data collected with the Forward Meson Spectrometer in transversely polarized $p^{\uparrow} + p$ collisions at $\sqrt{s} = 200$ GeV at STAR in 2015. We also explore the photon-multiplicity-dependent EM-jet A_N for single diffractive processes and rapidity gap events. The size of the EM-jet A_N for inclusive processes, single diffractive process and the rapidity gap events are consistent within uncertainty. These results do not provide evidence to show the single diffractive process contributes to large A_N in the inclusive processes.

31st International Workshop on Deep Inelastic Scattering (DIS2024)
8–12 April 2024
Grenoble, France

*Speaker

1. Introduction

Transverse single-spin asymmetry (A_N), also known as the left-right asymmetry, refers to the asymmetry in particle production concerning the plane defined by the momentum and spin directions of the polarized beam. Over the past few decades, numerous studies have observed significant A_N in charged- and neutral-hadron productions from polarized hadron-hadron collisions [1–5]. These findings contrast with the nearly zero A_N predicted by perturbative Quantum Chromodynamics in the hard scattering process [6]. Two major frameworks have been proposed to explain these sizeable asymmetries: the transverse-momentum dependent (TMD) formalism and the twist-3 factorization scheme. The TMD formalism introduces contributions from the initial-state quark and gluon Sivers functions and/or the final-state Collins fragmentation functions [7, 8], while the twist-3 factorization scheme involves contributions from the quark-gluon or gluon-gluon correlations and fragmentation functions [9]. Furthermore, recent studies at STAR suggest that the significant A_N might originate from diffractive processes [5, 10].

The STAR experiment is one of the major experiments at the Relativistic Heavy Ion Collider (RHIC) at Brookhaven National Laboratory. RHIC is the only polarized proton-proton collider in the world that can provide transversely or longitudinally polarized proton-proton collisions at $\sqrt{s}$ = 200 and 500/510 GeV. For the analyses presented in this talk, the data set from transversely polarized $p^{\uparrow} + p$ collisions at $\sqrt{s}$ = 200 GeV collected in 2015 is used. This data set features an average beam polarization of approximately 57% and an integrated luminosity of about 52 pb^{-1}.

2. Multi-dimensional inclusive EM-jet A_N for $p^{\uparrow} + p$ collisions at $\sqrt{s}$ = 200 GeV

The electromagnetic jets (EM-jets) for these analysis are the jets reconstructed using only photons detected at Forward Meson Spectrometer (FMS). Located on the west side of STAR apparatus, the FMS is an electromagnetic calorimeter designed to capture photons, neutral pions, and η mesons, covering the pseudo-rapidity range of 2.6 to 4.2 with full azimuthal coverage [11]. The anti-k_T algorithm was employed to reconstruct the EM-jets, with the resolution parameter of $R = 0.7$ [12]. To correct the reconstructed EM-jet energy and transverse momentum (p_T), the underlying event contribution was subtracted using the "off-axis" cone method [13]. Additionally, simulations were employed to account for the detector effects and correct the EM-jet kinematics to the "particle level". A minimum p_T threshold was applied to the EM-jets, determined to meet both the trigger threshold and the fixed threshold of $p_T > 2$ GeV/c.

The cross-ratio method was used to extract the A_N [14]. The left panel of Fig. 1 shows the preliminary plots for the multi-dimensional study of the inclusive EM-jet A_N as a function of photon multiplicity, EM-jet p_T, and EM-jet energy. For $x_F > 0$ (where x_F denotes the longitudinal momentum fraction $x_F = 2p_L/\sqrt{s}$), the A_N for the EM-jets decreases as the photon multiplicity increases, with the largest A_N observed for EM-jets containing 1 or 2 photons. Furthermore, the observed A_N remains consistent with zero for $x_F < 0$.

The right panel of Fig. 1 presents the inclusive EM-jet A_N as a function of x_F with a dependency on EM-jet photon multiplicity. The inclusive EM-jet A_N shows an increasing trend as x_F increases, regardless of the photon multiplicity. The A_N of the EM-jets for the case of 1 or 2 photon multiplicity also shows the largest values. Both plots in Fig. 1 indicate that the significant contributions to the observed A_N in inclusive processes may originate from diffractive processes. These observations motivate further exploration of the single diffractive EM-jet A_N.

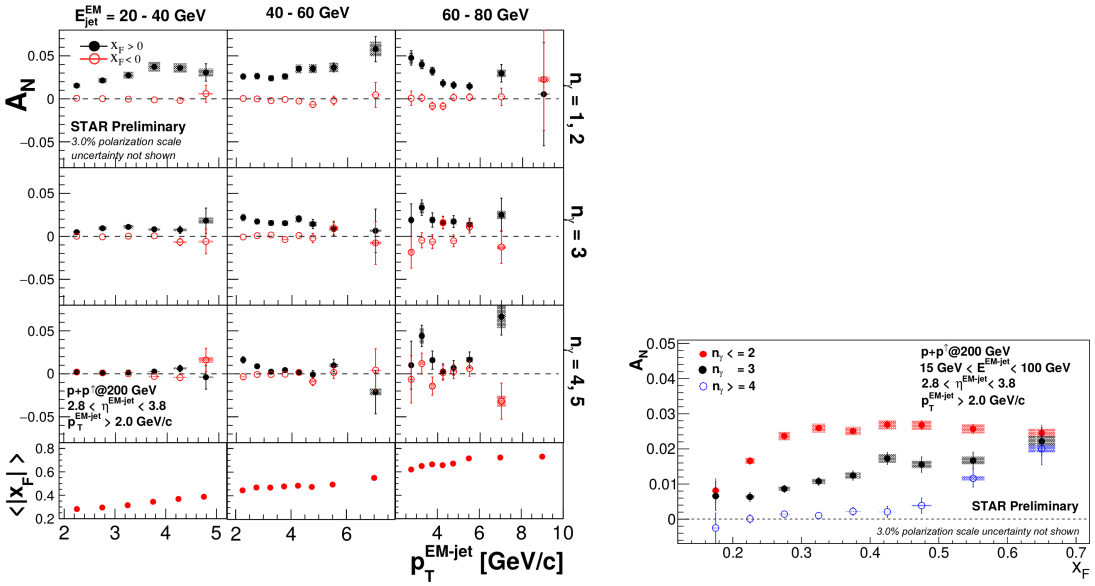

Figure 1: (left) A_N of inclusive EM-jets at $\sqrt{s}$ = 200 GeV sorted by EM-jet photon multiplicity, p_T, and energy bins. The lowermost panels display the average x_F values corresponding to each p_T bin. The black solid points represent the A_N values for $x_F > 0$ and the red hollow points depict the A_N values for $x_F < 0$. (right) Inclusive EM-jet A_N as a function of x_F at $\sqrt{s}$ = 200 GeV for three cases: $n_\gamma \leq 2$, $n_\gamma = 3$, $n_\gamma \geq 4$.

3. Single diffractive EM-jet A_N for $p^\uparrow + p$ collision at $\sqrt{s}$ = 200 GeV

For the single diffractive process, we consider events where only one EM-jet is detected by the FMS and only one proton track is detected by the east-side Roman Pot (RP). The Roman Pot detectors are designed to detect slightly scattered protons in close proximity to the beamline [15]. Additionally, a veto on east side Beam-Beam Counter (BBC) is applied by discarding the events with high ADC values on the east side BBC. Such a veto not only minimizes the accidental coincidences, but also helps establish the rapidity gap required for the single diffractive process, since the east side BBC covers the pseudorapidity range between -5 to -2.1, and it is situated between the FMS and east side RP.

The left panel of Fig. 2 shows the preliminary results for single diffractive EM-jet A_N as a function of x_F, categorized by three cases of EM-jet photon multiplicity. For $x_F > 0$, the single diffractive EM-jet A_N shows non-zero values with a significance greater than 2σ for both all photon multiplicities combined and for EM-jets with 1 or 2 photons. In addition, the A_N for EM-jets with 1 or 2 photon multiplicity is much larger than for EM-jets with 3 or more photons.

These events with east proton tagged, however, are the small fraction of the real single diffractive events due to the limited acceptance of the RP. Therefore, another category of events, with only one EM-jet at FMS and the veto on east BBC without any requirement on RP, is studied. These events are termed Rapidity Gap (RG) events because the veto on the east BBC still ensures a rapidity gap. More than 50 % of the RG events are the real single diffractive events. The right panel of Fig. 2 presents the preliminary results of the EM-jet A_N for the RG events. It shows that the size of the EM-jet A_N for the RG events is similar to the size of A_N for the inclusive events. Additionally, the A_N for EM-jets with 1 or 2 photon multiplicity is the largest.

To address whether the single diffractive process could contribute to the large A_N in the inclusive process, a direct comparison of EM-jet A_N in inclusive process, single diffractive process, and rapidity gap events is presented in Fig. 3. This figure shows that the EM-jet A_N values for the three processes are consistent with each other within the uncertainty. Given that the diffractive cross

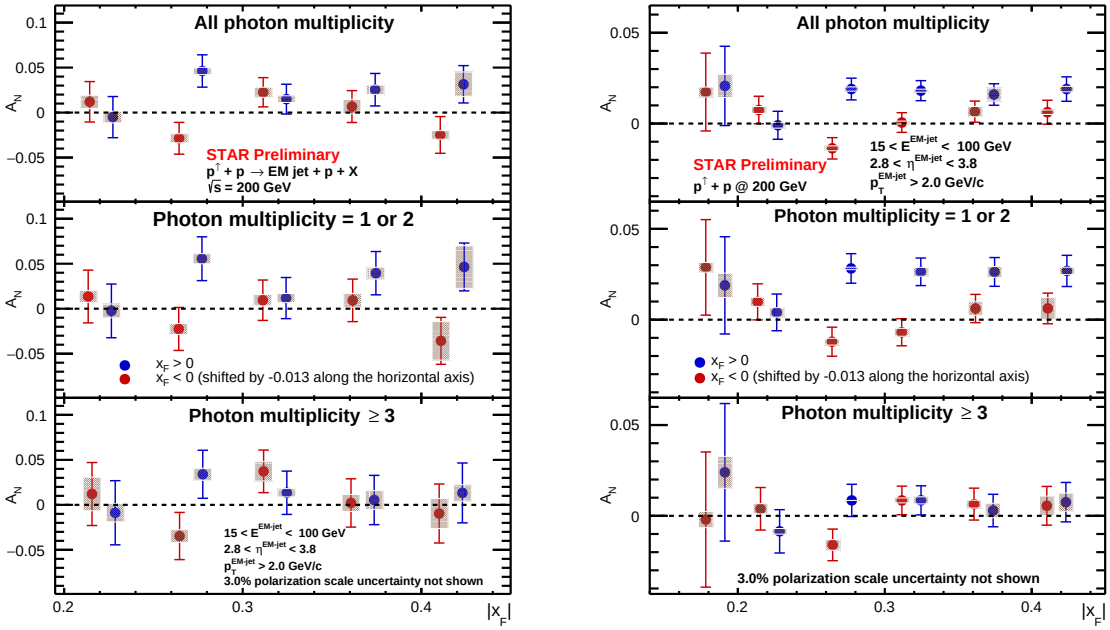

Figure 2: A_N of single diffractive process (left) and rapidity gap events (right) EM-jet at $\sqrt{s}$ = 200 GeV for three photon multiplicity cases: all photon multiplicity(top), photon multiplicity $\leq$ 2 (middle), photon multiplicity $\geq$ 3 (bottom). The blue points represent the A_N values for $x_F > 0$ and the red points depict the A_N values for $x_F < 0$.

section accounts for only about 20 % in the total inclusive cross section at the forward region, a large A_N would be expected for diffractive process if it had a dominant contribution in the large A_N in the inclusive processes [4]. However, such a large A_N is not observed in the single diffractive process. Therefore, the single diffractive process can not provide evidence to have significant contribution to large A_N in inclusive process.

4. Conclusion

We present the A_N for inclusive and single diffractive EM-jet using the FMS at STAR in $p^{\uparrow} + p$ collisions at $\sqrt{s}$ = 200 GeV. The inclusive EM-jet A_N exhibits an increasing trend with higher values of x_F and decreasing photon multiplicity, consistent with previous analyses at STAR. The A_N for single diffractive processes is shown to be non-zero with a significance of more than 2 σ for both all photon multiplicities combined and for 1 or 2 photon multiplicity. However, in the rapidity gap events, more than half of which are single diffractive, the size of the A_N is similar to that of the inclusive process. Furthermore, the EM-jets with 1 or 2 photon multiplicity explicit the largest A_N for all of these processes. Finally, a direct comparison plot of the EM-jet A_N for these three processes shows consistency in the A_N values. The presented measurement does not support diffractive processes as the dominant contributor to the large inclusive A_N in the forward rapidities.

References

[1] D.L. Adams *et al.*, Phys. Lett. B 261, 201(1991)

[2] B. I. Abelev *et al.* (STAR Collaboration), Phys. Rev. Lett. 101, 222001(2008)

[3] A. Adare *et al.* Phys. Rev. D 90, 012006 (2014)

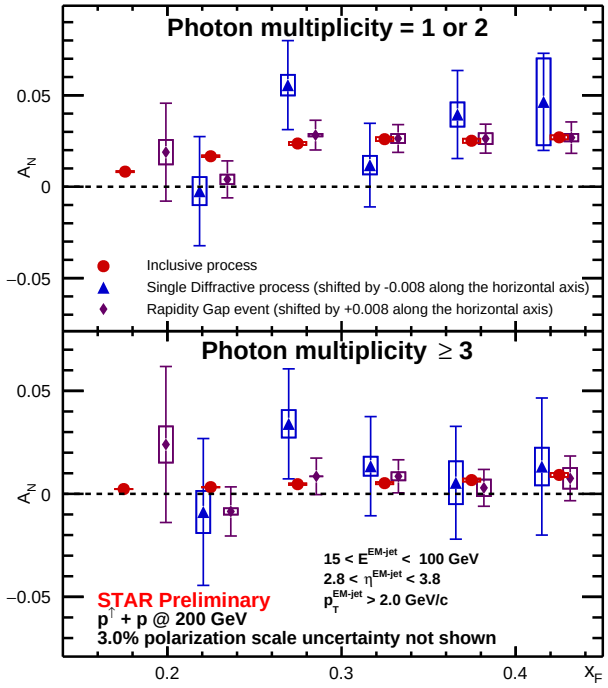

Figure 3: Comparison plot of the A_N for the EM-jets in inclusive processes, single diffractive process, and rapidity gap events as a function of x_F, categorized by photon multiplicity: ≤ 2 (top) and ≥ 3 (bottom). The red points represent the A_N for inclusive process; the blue points represent the A_N for single diffractive process with a constant shift of -0.008 along the x-axis for clarity; the purple points represent the A_N for rapidity gap events with a constant shift of +0.008 along the x-axis.

[4] E.C. Aschenauer *et al.*, arXiv:1602.03922

[5] J. Adam *et al.* (STAR Collaboration), Phys. Rev. D 103, 092009 (2021)

[6] G. L. Kane, J. Pumplin, and W. Repko. Phys. Rev. Lett. 41, 1689 (1978)

[7] D. Sivers, Phys. Rev. D 41, 83 (1990)

[8] J. Collins, Nucl Phys B 396 (1993) 161

[9] J.W. Qiu and G. Sterman, Phys. Rev. Lett. 67 2264 (1991)

[10] M.M. Mondal (STAR Collaboration) PoS (DIS2014) 216

[11] J. Adam *et al.* (STAR Collaboration), Phys. Rev. D 98, 032013 (2018)

[12] M.Cacciari, G. P. Salam, and G. Soyez, Eur. Phys. J. C (2012) 72: 1896

[13] B. B. Abelev *et al.* (ALICE Collaboration), Phys. Rev. D 91, 112012 (2015)

[14] X. Liang (STAR Collaboration) 10.5281/zenodo.7236716

[15] J. Adam *et al.* (STAR Collaboration), Phys. Lett. B 808 (2020) 135663